Journal of Photochemistry and Photobiology A: Chemistry 282 (2014) 16–24

Contents lists available at ScienceDirect

Journal of Photochemistry and Photobiology A: Chemistry

journal homepage: www.elsevier.com/locate/jphotochem

Synthesis and photodynamic properties of 5,10,15,20-tetrakis[3-(*N*-ethyl-*N*-methylcarbazoyl)]chlorin and its analogous porphyrin in solution and in human red blood cells

Darío D. Ferreyra, Mariana B. Spesia, M. Elisa Milanesio, Edgardo N. Durantini *

Departamento de Química, Facultad de Ciencias Exactas Físico-Químicas y Naturales, Universidad Nacional de Río Cuarto, Agencia Postal Nro. 3, X5804BYA Río Cuarto, Córdoba, Argentina

ARTICLE INFO

Article history:
Received 21 November 2013
Received in revised form 1 February 2014
Accepted 15 February 2014
Available online 25 February 2014

Keywords:
Chlorin
Carbazole
Photodynamic activity
Erythrocytes
Photohemolysis

ABSTRACT

The spectroscopic and the photodynamic properties of 5,10,15,20-tetrakis[3-(*N*-ethyl-*N*-methylcarbazoyl)]chlorin (TEMCC) and its analogous porphyrin (TEMCP) were investigated in *N*,*N*-dimethylformamide (DMF) and in human red blood (HRB) cells. A more intense absorption band at 650 nm was obtained for TEMCC in comparison with TEMCP. Both photosensitizers showed red fluorescence emission with quantum yields of 0.13 and 0.23 for TEMCP and TEMCC, respectively. The photodynamic activity of TEMCC was higher that TEMCP in DMF, with a quantum yield of singlet molecular oxygen of 0.49. Moreover, in presence of NADH these photosensitizers produced superoxide anion radical. *In vitro* experiments showed that TEMCC was a highly effective agent to hemolyze the HRB cells. A decrease in the HRB cells osmotic stability was observed after photodynamic treatment with TEMCC. Studies of photodynamic action mechanism showed that the photohemolysis of HRB cells was protected in the presence of azide ion. Also, a reduction on the cell photodamage was found using mannitol. In contrast, the photohemolytic effect considerably increased in D_2O. Therefore, the photodynamic activity of TEMCC in HRB cells was mediated by a contribution of type I and type II photooxidative mechanisms.

1. Introduction

Photodynamic therapy (PDT) is based on the action of visible light on a phototherapeutic agent in presence of oxygen, resulting in the production of reactive oxygen species (ROS) and the subsequent destruction of tumor cells [1]. Thus, PDT is a promising treatment modality for several diseases, most notably cancer. Finding a suitable photosensitizer is crucial in improving the efficacy of PDT. A large number of potential photosensitizers for PDT have been proposed for different pathological conditions. Most photosensitizers used in PDT are cyclic tetrapyrroles, comprising substituted derivatives of porphyrin, chlorin, and bacteriochlorin [2]. However, acceptable photosensitizers for PDT must present specific chemical and biological properties [3]. Two of the photochemical requisites are a high absorption coefficient in the visible region of the spectrum and a long lifetime of triplet excited state to produce efficiently ROS. In this approach visible light is used to activate a photosensitizer, which can react with molecules from its direct environment by electron or hydrogen transfer, leading to the production of radicals (type I reaction), or it can transfer its energy to oxygen, generating the highly reactive singlet molecular oxygen, $O_2(^1\Delta_g)$ (type II reaction). These mechanisms can take place at the same time and the contribution of the two processes is affected by the photosensitizer, substrate and the microenvironment surrounding the agent [4].

The properties of chlorins often satisfy the demands of a good photosensitizer, and therefore they are strong candidates for better photosensitizers. *In vivo* applications of porphyrin derivatives are hampered by their spectroscopic characteristics, which do not feature absorption in the red region. These photosensitizers exhibit an intense Soret absorption band around 420 nm and a lower bands at 510–650 nm. Therefore, porphyrins are only activated by wavelengths with limited tissue penetration. However, porphyrins can be converted to the corresponding chlorin derivatives, which show an intense absorption band at 650 nm [5]. Thus, 5,10,15,20-tetrakis(3-hydroxyphenyl)chlorin is one of the oldest examples for a second generation of photosensitizers and, next to Photofrin, presents one of the most widely studied drugs in PDT and

* Corresponding author. Tel.: +54 358 4676157; fax: +54 358 4676233.
E-mail address: edurantini@exa.unrc.edu.ar (E.N. Durantini).

http://dx.doi.org/10.1016/j.jphotochem.2014.02.004
1010-6030/

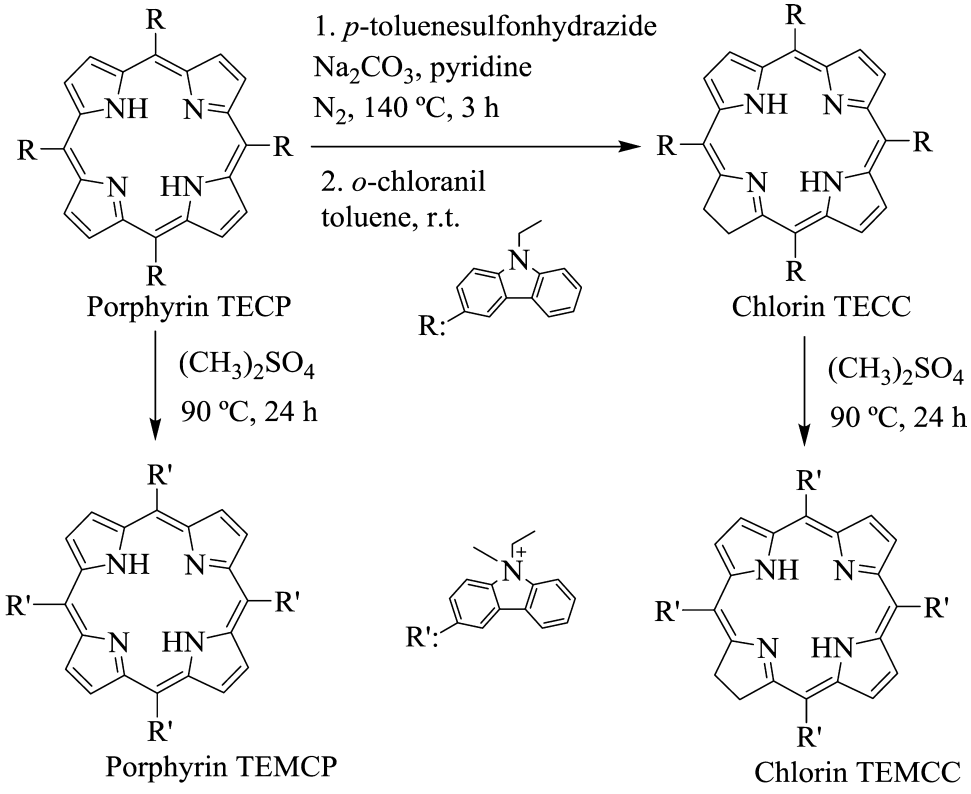

Scheme 1. Synthesis of porphyrin and chlorin derivatives.

photodiagnostics [6]. Simple modifications of the *m*THPP framework have been used to prepare a variety of related derivatives. Chlorin e_6 has been most frequently used as an anionic photosensitizer for PDT. Especially for chlorin e_6 derivatives many targeted bioconjugates were prepared and the nuclear targeting resulted in an increase in PDT effects [1].

In this work, a novel tetracationic chlorin, 5,10,15,20-tetrakis[3-(*N*-ethyl-*N*-methylcarbazoyl)]chlorin (TEMCC), was synthetized from the analogous porphyrin derivative. TEMCC contains four carbazoyl groups at the *meso* positions. Many condensed heterocyclic compounds containing a carbazole nucleus have been reported to develop a broad range of potent biological activities, notably anticancer activity [7]. In addition, the nitrogen atom in the carbazole unit can be methylated to produce cationic groups on the periphery of the macrocycle. Cationic porphyrins have several interesting features which make these compounds attractive photosensitizers for a variety of biological systems [8]. Therefore, in the present investigation the spectroscopic and photodynamic properties of TEMCC were compared with those obtained for 5,10,15,20-tetrakis[3-(*N*-ethyl-*N*-methylcarbazoyl)]porphyrin (TEMCP) in solution and in human red blood (HRB) cells. Cell membranes seem to be important targets for many antineoplastic photosensitizer agents. In this sense, mammalian erythrocytes serve as convenient model cells for exploration of physiological and molecular mechanisms involved in PDT [9,10].

2. Materials and methods

2.1. General

Absorption and fluorescence spectra were recorded on a Shimadzu UV-2401PC spectrometer (Shimadzu Corporation, Tokyo, Japan) and on a Spex FluoroMax spectrofluorometer (Horiba Jobin Yvon Inc., Edison, NJ, USA), respectively. Proton nuclear magnetic resonance spectra were recorded on a FT-NMR Bruker Avance DPX400 spectrometer at 400 MHz. Mass Spectra were taken with a Bruker micrO-TOF-QII (Bruker Daltonics, MA, USA) equipment with an ESI source operated in positive/negative mode, using nitrogen as nebulizing and drying gas and sodium formiate (10 mM) as internal calibrant. The visible light source used to irradiate HRB cell suspensions was a Novamat 130 AF (Braun Photo Technik, Nürnberg, Germany) slide projector equipped with a 150 W lamp. The light was filtered through a 2.5 cm glass cuvette filled with water to absorb heat. A wavelength range between 350 and 800 nm was selected by optical filters. The light intensity at the treatment site was 30 mW/cm^2 (Radiometer Laser Mate-Q, Coherent, Santa Clara, CA, USA). Microscopic observations were performed in a Carl Zeiss Axiostar plus, transmitted-light microscope (Götingen, Germany).

All the chemicals from Aldrich (Milwaukee, WI, USA) were used without further purification. Silica gel thin-layer chromatography (TLC) Plates 250 microns from Analtech (Newark, DE, USA) were used. Solvents (GR grade) from Merck (Darmstadt, Germany) were distilled. Ultrapure water was obtained from a Labconco (Kansas, MO, USA) equipment model 90901-01.

2.2. Photosensitizers

5,10,15,20-Tetrakis(4-methoxyphenyl)porphyrin (TMPP) was purchased from Aldrich. 5,10,15,20-Tetrakis[3-(*N*-ethylcarbazoyl)]porphyrin (TECP) was synthesized as previously described [11]. Synthesis procedures of porphyrin and chlorin derivatives are summarized in Scheme 1.

5,10,15,20-Tetrakis[3-(*N*-ethylcarbazoyl)]chlorin (TECC). A solution of TECP (37 mg, 0.034 mmol) and Na_2CO_3 (1.50 g, 0.015 mol) was prepared in pyridine (25 mL). Then, a solution of de *p*-toluenesulfonhydrazide (372 mg, 2 mmol) in pyridine (5 mL) was added under an argon atmosphere. The reaction mixture was stirred and heated to 140 °C for 3 h. After cooling at room

Table 1
Spectroscopic and photodynamic properties of photosensitizers in DMF.

Photosensitizer	ε^{Soret} [a]	ε^{QI} [a]	Φ_F [b]	k_{obs}^{DMA} (s^{-1})[c]	Φ_Δ [d]
TMPP	1.81×10^5	4.8×10^3	0.14 ± 0.02	$(9.9 \pm 0.3) \times 10^{-4}$	0.65 ± 0.02
TECP	2.81×10^5	7.0×10^3	0.14 ± 0.02	$(5.6 \pm 0.3) \times 10^{-4}$	0.37 ± 0.02
TECC	1.25×10^5	21.5×10^3	0.25 ± 0.02	$(5.2 \pm 0.3) \times 10^{-4}$	0.36 ± 0.02
TEMCP	2.80×10^5	5.9×10^3	0.13 ± 0.02	$(6.1 \pm 0.2) \times 10^{-4}$	0.40 ± 0.02
TEMCC	1.24×10^5	17.0×10^3	0.23 ± 0.02	$(7.6 \pm 0.3) \times 10^{-4}$	0.49 ± 0.02

[a] Molar absorption coefficient ($L\,mol^{-1}\,cm^{-1}$).
[b] Fluorescence quantum yield.
[c] Observed rate constants for the photooxidation reaction of DMA.
[d] Quantum yield of $O_2(^1\Delta_g)$ production.

temperature, the crude mixture was treated with toluene (50 mL) and water (50 mL). The organic phase was separated and washed with HCl (3 M, 25 mL), water (25 mL) and saturated water solution of $NaHCO_3$. The presence of chlorin and bacteriochlorin was monitored by UV-visible spectroscopy (bands at 654 and 742 nm, respectively). *o*-Chloranil (6 mg, 0.024 mmol) was slowly added to the stirred organic solution at room temperature until the absorption peak at 742 nm (bacteriochlorin) disappeared. The solvent was evaporated under vacuum. The residue was purified by flash column chromatography (silica gel, chloroform/*c*-hexane/TEA: 80/19.8/0.2) to yield 35 mg (95%) of TECC. TLC (silica gel, chloroform/*c*-hexane/TEA: 80/19.8/0.2) $R_f = 0.74$. ^{1}HNMR ($CDCl_3$, TMS) δ [ppm] −1.12 (bs, 2H, NH—pyrrole), 1.64 (t, 12H, $J = 7.0$ Hz, —CH_3), 4.23 (s, 4H, —CH_2—pyrrole), 4.59 (q, 8H, $J = 7.0$ Hz, —CH_2—), 7.27 (m, 4H), 7.50–7.59 (m, 8H), 7.67–7.72 (m, 4H), 7.98–8.03 (m, 2H), 8.22 (d, 2H, $J = 4.8$ Hz, CH—pyrrole), 8.47 (s, 2H, CH—pyrrole), 8.61 (d, 2H, $J = 4.8$ Hz, CH—pyrrole). ESI-MS [*m*/*z*] 1085.5019 $(M+H)^+$ (1084.4941 calculated for $C_{76}H_{60}N_8$).

5,10,15,20-Tetrakis[3-(*N*-ethyl-*N*-methylcarbazoyl)]chlorin (TEMCC). A solution of TECC (35 mg, 0.032 mmol) and dimethyl sulphate (1.75 mL) was heated to 90 °C with stirring under argon atmosphere for 24 h. The mixture was cooled and the product was precipitated with ether. The solid was separated by centrifugation and washed with ether, Na_2CO_3 (2%, w/v) and water yielding 44 mg (92%) of TEMCC. ^{1}HNMR (DMSO-d_6, TMS) δ [ppm] −1.25 (bs, 2H, NH—pyrrole), 1.54 (t, 12H, $J = 7.0$ Hz), 2.90 (s, 12H), 4.27 (s, 4H, —CH_2—pyrrole), 7.60–9.10 (m, 34H, carbazole and CH—pyrrole). ESI-MS [*m*/*z*] 1145.5958 $(M+H)^+$ (1144.5858 calculated for $C_{80}H_{72}N_8$).

5,10,15,20-Tetrakis[3-(*N*-ethyl-*N*-methylcarbazoyl)]porphyrin (TEMCP). Methylation of TECP was performed as described above for TEMCC, using TECP (11 mg, 0.010 mmol) to obtain 13 mg (96%) of TEMCP. ^{1}HNMR (TMS) δ [ppm] −2.56 (bs, 2H, NH—pyrrole), 1.59 (t, 12H, $J = 7.1$ Hz, —CH_3), 2.90 (s, 12H), 7.62–9.15 (m, 36H, carbazole and CH—pyrrole). ESI-MS [*m*/*z*] 1143.5802 $[M+H]^+$ (1142.5701 calculated for $C_{80}H_{70}N_8$).

Stock solutions (0.5 mM) of photosensitizers were prepared by dissolution in 1 mL of *N*,*N*-dimethylformamide (DMF). The concentrations were checked by spectroscopy, taking into account the values of molar absorption coefficients (Table 1).

2.3. Spectroscopic studies

Absorption and fluorescence spectra were recorded in a quartz cell of 1 cm path length at 25.0 ± 0.5 °C. The fluorescence quantum yield (Φ_F) of the photosensitizers was calculated by comparison of the area below the corrected emission spectrum in DMF with that of TMPP as a reference. A value of $\Phi_F = 0.14$ for TMPP in DMF was calculated by comparison with the fluorescence spectrum in tetrahydrofuran using $\Phi_F = 0.14$ and taking into account the refractive index of the solvents [12]. Sample and reference absorbances (>0.05) were matched at the excitation wavelength (522 nm) and the areas of the emission spectra were integrated in the range 600–800 nm.

2.4. Steady state photolysis

Solutions of 9,10-dimethylanthracene (DMA, 35 μM) and photosensitizer in DMF were irradiated in 1 cm path length quartz cells (2 mL) with monochromatic light at $\lambda_{irr} = 427$ nm (photosensitizer absorbance 0.1), from a Cole-Parmer illuminator 41720-series (Cole-Parmer, Vernon Hills, IL, USA) with a 150 W halogen lamp through a high intensity grating monochromator (Photon Technology Instrument, Birmingham, NJ, USA). The light fluence rate was determined as 0.35 mW/cm^2. The kinetics of DMA photooxidation were studied by following the decrease of the absorbance (*A*) at $\lambda_{max} = 378$ nm. The observed rate constants (k_{obs}) were obtained by a linear least-squares fit of the semilogarithmic plot of $\ln A_0/A$ *vs.* time. Quantum yields of $O_2(^1\Delta_g)$ production (Φ_Δ) were calculated comparing the k_{obs} for the corresponding photosensitizer with that for TMPP, which was used as a reference ($\Phi_\Delta = 0.65$) [12]. Measurements of the sample and reference under the same conditions afforded Φ_Δ for photosensitizers by direct comparison of the slopes in the linear region of the plots.

2.5. Detection of superoxide anion radical

The nitro blue tetrazolium (NBT) method was used to detect superoxide anion radical ($O_2^{\bullet -}$) formation in DMF [13,14]. The NBT method was carried out using 0.2 mM NBT, 0.5 mM NADH and photosensitizer (absorbance 0.3 at Soret band) in 2 mL of DMF/water (9/1). Control experiments were performed in absence of NBT, NADH or photosensitizer. Samples were irradiated in 1 cm path length quartz cells under aerobic condition with visible light from the Cole-Parmer illuminator 41720-series filtered through a 2.5 cm glass cuvette filled with water (44 mW/cm^2). The progress of the reaction was monitored by following the increase of the absorbance at λ = 560 nm.

2.6. Studies in HRB cells

HRB cells were obtained from healthy donors. After extraction, the whole blood was taken into anticoagulant EDTA, centrifuged (3000 rpm for 5 min) to remove plasma and the leukocyte layer, washed three times with phosphate buffer saline (PBS) solution (137 mM NaCl, 2.7 mM KCl, 1.5 mM KH_2PO_4 and 8 mM Na_2HPO_4) and centrifuged again. HRB cells were re-suspended in saline solution (0.9%, w/v, NaCl) to get a cellular density of ~10^6 cells/mL and maintained at 4 °C until use [15].

2.6.1. Photohemolysis assays

HRB cell suspensions (2 mL, ~10^6 cells/mL) were placed in Pyrex brand culture tubes (13 mm × 100 mm) and incubated with different concentrations (4–10 μM) of photosensitizer in dark for 30 min at 37 °C. Photosensitizers were added from a 0.5 mM stock

solution in DMF. After incubation HRB cells suspensions were irradiated with visible light as described above. After irradiation, the samples were kept 24 h at 4 °C in dark. Then, the tubes were centrifuged (3000 rpm for 5 min) and 100 μL of supernatants were diluted in 2 mL of distilled water. The hemoglobin content was determined by measuring the absorbance at 413 nm. Results are expressed as percentage of hemolysis taking 100% as the absorbance obtained from a sample lysed in distilled water [15]. Similar experiments were performed in presence of sodium azide (50 mM) or mannitol (50 mM), which were added to HRB cell suspensions from 2.5 M stock solutions in water and the cells were incubated for 30 min at 37 °C in dark together with 4 μM TEMCC. For photohemolysis assays in D_2O, HRB cells (2 mL) were centrifuged (3000 rpm for 5 min) and re-suspended in 2 mL solution of 0.9%, w/v, NaCl in D_2O. This flask was incubated for 30 min at 37 °C in dark for cells adaptation. Then, HRB cells were centrifuged again and resuspended in a new solution of 0.9%, w/v, NaCl in D_2O. Cells were incubated with 4 μM TEMCC for 30 min at 37 °C in dark. After that, samples were irradiated as described above.

2.6.2. Osmotic fragility evaluation

Suspensions of HRB cells (2 mL, ~10^6 cells/mL) were treated with 4 μM TEMCC as described above and irradiated for 2 min with visible light. After that 100 μL of HRB cells suspension were diluted in NaCl solution (2 mL) of various concentrations (0.2–0.9%, w/v). Then, the suspensions were incubated for 24 h at 4 °C in dark. Then, the samples were centrifuged (3000 rpm for 5 min) and the percentage of osmotically lysed cells was estimated as previously described [16].

2.6.3. Micrographs of photohemolysis

Suspensions of HRB cells (2 mL, ~10^6 cells/mL) were incubated with 4 μM TEMCC as previously indicated. The samples were observed under microscope using 100× objective and they were irradiated with visible light from the microscope light source. Imagines were recorded every 5 min.

2.7. Controls and statistical analysis

In all studies using HRB cells, control experiments were carried out without illumination in the absence and presence of photosensitizer and irradiating the HRB cells without photosensitizer. Each experiment was repeated separately three times. The unpaired *t*-test was used to establish the significance of differences between groups. Differences were considered statistically significant with a confidence level of 95% ($p < 0.05$) considered statistically significant. Data were represented as the mean ± standard deviation of each group.

3. Results and discussion

3.1. Synthesis of chlorin derivatives

A novel chlorin TECC substituted in the *meso* position by four carbazoyl groups was synthesized from porphyrin TECP by a two-step procedure (Scheme 1). First, the tetrapyrrolic macrocycle of TECP was reduced with *p*-toluenesulfonhydrazide. This approach produced a mixture of TEPC and the corresponding bacteriochlorin. The reaction was carried out until the relationship between the absorbance of the bacteriochlorin band at 742 nm and chlorine Soret band 420 nm remained constant. Fig. 1 shows the absorption spectra at the beginning and end of the reaction. In a second step, *o*-chloranil was used as selective oxidant to obtain TECC. The reaction mixture in toluene was stirred until bacteriochlorin absorption peak at 742 nm disappeared. The product was isolated with 95% yield. These chlorin TECC and porphyrin TECP were employed to

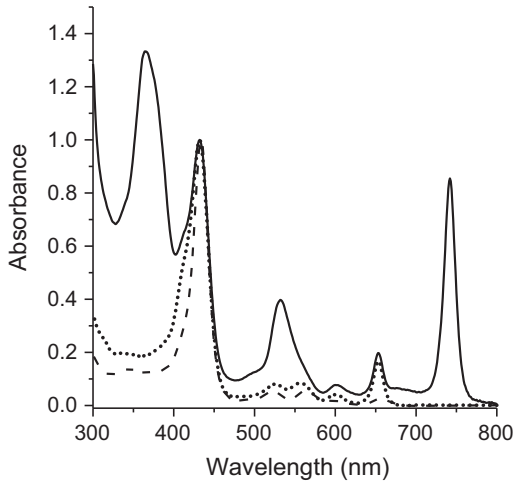

Fig. 1. Absorption spectra of reaction mixtures (solid line), TECP (dashed line) and TECC (dotted line) in DMF.

synthesize tetracationic photosensitizers (Scheme 1). Thus, TECC and TECP were treated with dimethyl sulphate to obtain TEMCC and TEMCP with 92 and 96% yield, respectively. Thus, the presence of four cationic charges on the chlorin macrocycle could facilitate the interaction with the biological membrane [16].

3.2. Absorption and fluorescence spectroscopic studies

Absorption spectra of TEMCC and TEMCP were studied in DMF (Fig. 2A). The spectra show a higher intensity band around ~430 nm (Soret band), with molar absorption coefficient values in the range of ~10^5 L mol^{-1} cm^{-1} (Table 1). Non-metallated *meso*-phenyl substituted porphyrins exhibit a characteristic Soret band at ~420 nm [12]. The bathochromic shift observed for TEMCP and TEMCC is due to an extension in the π conjugation produced by the carbazoyl groups in the macrocycle periphery. Also, these photosensitizers exhibit four bands of lower intensity in the visible region between 500 and 700 nm (Q-bands). The relative intensities of the Q-bands of TEMCP show a spectrum of the type *etio* ($\varepsilon_{IV} > \varepsilon_{III} > \varepsilon_{II} > \varepsilon_{I}$). In contrast, the Q-bands intensities of TEMCC following the sequence $\varepsilon_{I} > \varepsilon_{VI} - \varepsilon_{III} > \varepsilon_{II}$, with an intense $Q_x(0–0)$ band of about 10^4 L mol^{-1} cm^{-1}. As can be observed in Fig. 1, similar pattern in the absorption spectra was observed for TECP and TECC (Table 1). Therefore, both chlorin derivatives, TMCC and TEMCC, present the expected increase in absorbance of the $Q_x(0–0)$ band with the reduction of the porphyrin ring [17].

Fig. 2B shows the steady-state fluorescence emission spectra of TEMCC and TEMCP in DMF. Spectra present two bands in the region of 650–750 nm. These emission bands in the red spectral region are characteristic of chlorin and porphyrin derivatives [12,17]. From the intersection of the absorption and fluorescence spectra of the $Q_x(0–0)$ band, Stokes shifts of 3 and 9 nm were calculated for TEMCC and TEMCP, respectively. Small Stokes shifts indicated that in these molecules the spectroscopic energies are identical to the relaxed energies of the singlet state, according to the rigid planar structure of the tetrapyrrolic macrocycle. That suggests that only a minor geometric relaxation occurs in the first excited state. Fluorescence quantum yields (Φ_F) of these compounds were calculated in DMF by evaluation with TMPP as a reference (Table 1). The values of Φ_F agree with previously reported for similar porphyrin derivatives and they are appropriated for quantification of photosensitizers by fluorescence emission techniques [12]. Moreover, the fluorescence excitation spectra of TEMCC and TEMCP were compared in DMF (Fig. 2C), monitoring the emission at 720 nm. Excitation spectra of these compounds resemble the absorption spectra (Fig. 2A),

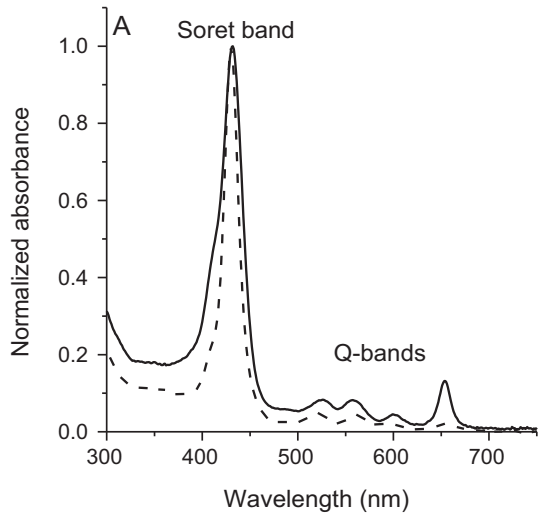

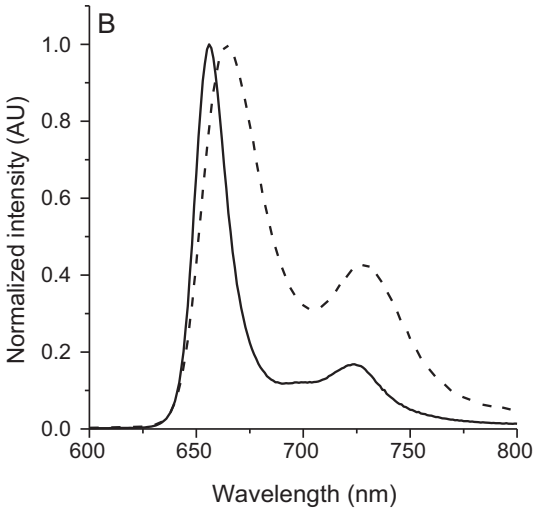

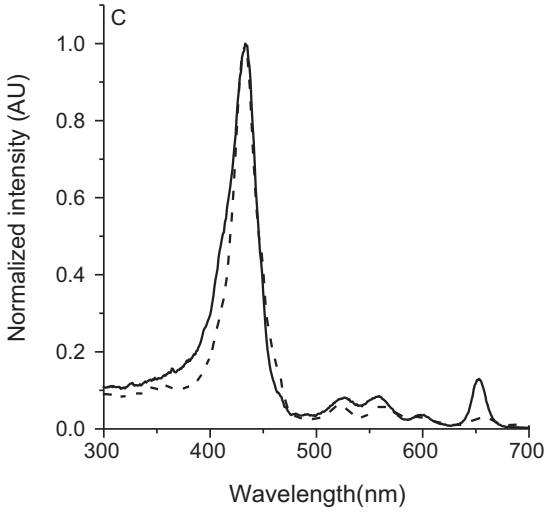

Fig. 2. (A) Absorption, (B) fluorescence emission (λ_{exc} = 525 nm) and (C) excitation (λ_{em} = 720 nm) spectra of TEMCC (solid line) and TEMCP (dashed line) in DMF.

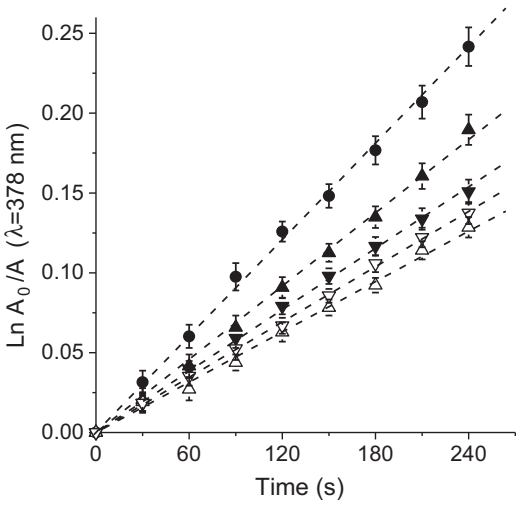

Fig. 3. First-order plots for the photooxidation of DMA photosensitized by TEMCC (▲), TEMCP (▼), TECC (△), TECP (▽) and TMPP (•) in DMF. Values represent mean ± standard deviation of three separate experiments.

indicating that these photosensitizers are essentially unaggregated in DMF.

3.3. Photodynamic activity in DMF solution

Photooxidation of DMA sensitized by porphyrin and chlorin derivatives was investigated in DMF under aerobic condition (Fig. 3). Values of the observed rate constant (k_{obs}^{DMA}) were calculated from first-order kinetic plots of the DMA absorption at 378 nm *vs*. time (Table 1). In all cases, similar rates of DMA decomposition were obtained, only slightly higher for the reaction photosensitized by TEMCC. Because DMA quenches $O_2(^1\Delta_g)$ by chemical reaction, photooxidation of this substrate was used as a method to evaluate the ability of the photosensitizers to produce $O_2(^1\Delta_g)$ in solution [18]. Thus, the quantum yield of $O_2(^1\Delta_g)$ production (Φ_Δ) was calculated by comparing the k_{obs}^{DMA} value for each photosensitizers with that for the reference (TMPP). Similar values of Φ_Δ were obtained for TECP, TECC and TEMCC, while a value slightly higher was found for TEMCC in DMF (Table 1). Thus, the production of $O_2(^1\Delta_g)$ induced by these compounds is quite reasonable to be used as phototherapeutic agents [19]. However, the values of Φ_Δ can significantly change in a different medium, diminishing mainly when the photosensitizer is not dissolves as monomer [20].

On the other hand, generation of $O_2^{\bullet-}$ was detected by NBT reduction to diformazan in presence of NADH, following the absorption at 560 nm in DMF (Fig. 4). Under aerobic conditions, it was prove that the photosensitized decomposition of NBT occurred predominantly through a type I photoreaction process [13]. The increase of diformazan absorption was monitored as a function of time after irradiation of samples with visible light. As shown in Fig. 4, reduction of NBT by $O_2^{\bullet-}$ was not detected in the photoirradiated samples without NADH. The effect of light irradiation on the decomposition of NBT considerably increases in presence of TEMCC or TEMCP and NADH with respect to solution without the photosensitizer derivatives. These results indicate an important contribution of the photodynamic activity induced by TEMCC and TEMCP in the diformazan production. Therefore, even though $O_2(^1\Delta_g)$ can be generated effectively by photoexcited photosensitizer triplet state of TEMCC and TEMCP, it was found that $O_2^{\bullet-}$ can also be generated especially in the presence of NADH. However, the photophysics of the photosensitizers established in solution can be significantly modified in a biological microenvironment. This limits to predict the photodynamic efficiency of a photosensitizer

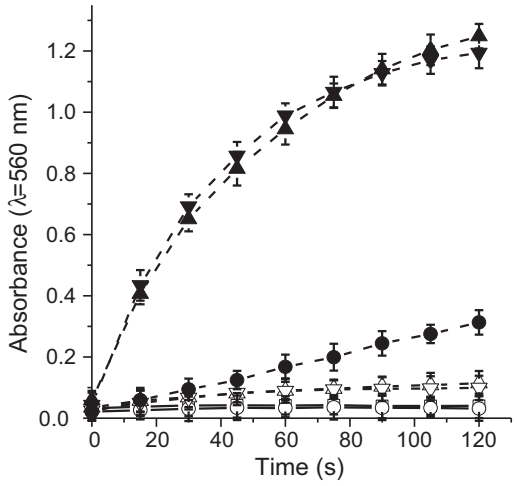

Fig. 4. Time course of $O_2^{\bullet -}$ generation detected by the NBT method as an increase in the absorption at 560 nm. Samples contain: TEMCC, NTB and NADH (▲); TEMCP, NTB and NADH (▼); TEMCC and NTB (△); TEMCP and NBT (▽); TEMCC and NADH (□); TEMCP and NADH (○); NADH and NBT (●) in DMF; [NBT] = 0.2 mM and [NADH] = 0.5 mM. Values represent mean ± standard deviation of three separate experiments.

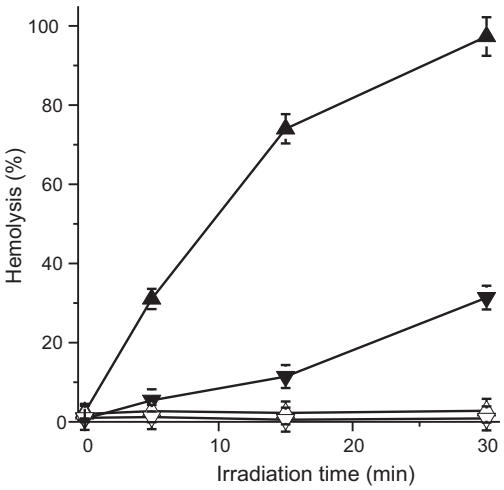

Fig. 6. Photohemolysis of HRB cells (~10^6 cells/mL) treated with 4 μM TEMCC (▲) and TEMCP (▼) for 30 min in dark and irradiated with visible light for different times in 0.9%, w/v, NaCl solution. HRB cells control treated with different concentration of TEMCC (△) and TEMCP (▽) for 30 min in dark and non-irradiated. Values represent mean ± standard deviation of three separate experiments.

in biological media only based on photophysical investigations in homogeneous medium.

3.4. Photohemolysis of HRB cells

In agreement with cell-culture assays, where cell death is monitored by membrane disruption, hemolysis of HRB cells can be used as a mode of measuring death of erythrocytes [9,21]. Hemoglobin absorption spectrum shows an intense Soret band at 413 nm and two Q-bands at 500–600 nm [15]. In this way, chlorins are appropriated photosensitizers in presence of blood because they absorb in the phototherapeutic window. Therefore, the photodynamic activity of TEMCC and TEMCP was evaluated *in vitro* by the photohemolytic effect on HRB cells (Fig. 5). Suspensions of HRB cells (~10^6 cells/mL) in saline solution were treated with different concentration of photosensitizer (4 and 10 μM) for 30 min at room temperature in dark. After 24 h without irradiation, negligible hemolysis was found for TEMCP indicating no dark toxicity induced by this porphyrin at 4 μM concentration. A slight increase in the hemolytic effect was found increasing the TEMCC concentration, reaching a 10% when cells were incubated with 10 μM in dark. In contrast, irradiation for 30 min with visible light without photosensitizer did not produce photohemolysis (data not shown). Therefore, the hemolysis obtained after irradiation of the HRB cells incubated with the photosensitizer for 30 min in dark (see Fig. 5) was due to the photodynamic activity of the agent. After 15 min irradiation with visible light, HRB cells treated with 10 μM TEMCC were completely hemolyzed, while TEMCP induced a 40% of hemolysis (Fig. 5). Also, using 4 μM TEMCC, which was nontoxic in dark, the photohemolysis reached a 75%. Therefore, the consequent cellular photohemolytic activities produced by TEMCC and TEMCP were compared using 4 μM and different irradiation periods. As can be observed in Fig. 6, the photohemolysis after HRB cells irradiation with visible light was dependent upon the photosensitizer structure and light exposure level. The photohemolysis produced by TEMCC was always higher than TEMCP. TEMCC induced a 31% of cellular lysis after 5 min of irradiation, while a similar phototoxic activity was found for TEMCP but after 30 min irradiation. In contrast, a 30 min irradiation induced complete lysis of the cells treated with the chlorin derivative. In all cases, TEMCC was more effective photosensitizer than TEMCP. The increase in the photohemolytic activity induced by TEMCC with respect to its porphyrin analogous can be due to its higher absorption at 653 nm, where hemoglobin does not absorb and the ε of TEMCC is ~3 times higher than TEMCP.

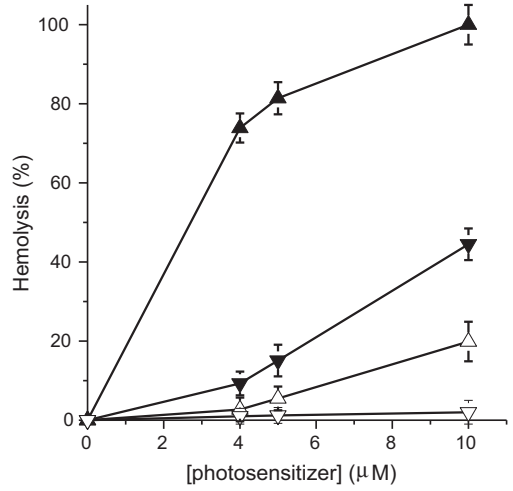

Fig. 5. Photohemolysis of HRB cells (~10^6 cells/mL) treated with different concentration of TEMCC (▲) and TEMCP (▼) for 30 min in dark and irradiated with visible light for 15 min in 0.9%, w/v, NaCl solution. HRB cells control treated with different concentration of TEMCC (△) and TEMCP (▽) for 30 min in dark and non-irradiated. Values represent mean ± standard deviation of three separate experiments.

3.5. Osmotic fragility of HRB cells

The membrane fragility of HRB cells was evaluated after photodynamic treatment with TEMCC. Osmotic fragility curves of erythrocytes treated with 4 μM TEMCC and irradiated for 2 min with visible light are shown in Fig. 7. This irradiation time was selected to produce a partial damage (~20%) in the HRB cells at NaCl concentration of 0.9%, w/v. The results indicate that the irradiation of HRB cells in the presence of TEMCC produced an increase in the HRB cells osmotic fragility. Thus, the concentration of NaCl corresponding to 50% osmotic hemolysis of native HRB cells was about 0.50%, w/v, NaCl, whereas that corresponding to cells treated with TEMCC was 0.62%.

The morphology of HRB cells was observed by microscopy after different irradiation times, using the visible light from the

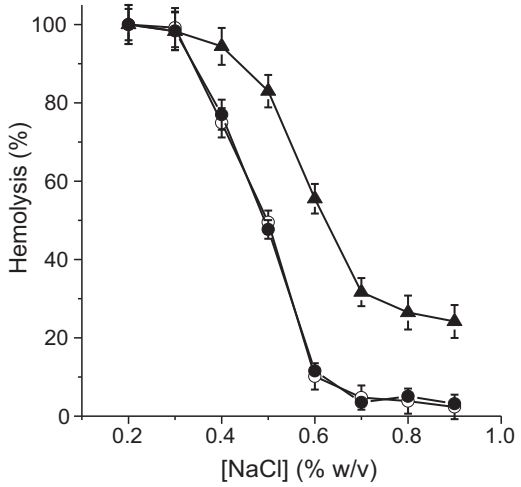

Fig. 7. Osmotic fragility of HRB cells (~10^6 cells/mL) incubated with 4 μM TEMCC (▲) for 30 min in dark and irradiated for 2 min with visible light (30 mW/cm^2). After irradiation the HRB cells were immediately washed and incubated for 30 min in different NaCl solutions. HRB cells control untreated and irradiated (●) and treated with TEMCC in dark (○). Values represent mean ± standard deviation of three separate experiments.

microscope light source. This experimental setup allowed keeping fixed field, observing the same group of cells after each period. Morphological changes of HRB cells without TEMCC and treated with 4 μM TEMCC were compared after each irradiation period. Representative results are shown in Fig. 8. The total irradiation time was of 20 min and the photographs were taken each 5 min. No changes were found in untreated HRB cells even after 20 min irradiation (Fig. 8 left column). However, variations in the shape and size of cells were observed in presence of TEMCC (Fig. 8 right column). Also, similar effect was present in all studied samples irradiated with visible light form the projector (results not shown).

These results provided evidence about membrane deformation and an increase in the volume of cells indicating a higher fragility after the photodynamic action. Similar deformation of membrane has been previously found in oxidative damage of HRB cells [22]. Photosensitized injure of HRB cells produces a significant increase of membrane fluidity due to the formation of defects in HRB cell membrane. This effect decreases erythrocytes osmotic stability and release the hemoglobin. In addition, the microscope images show changes in the HRB cells, when they are irradiated in the presence of the TEMCC. At the end of the irradiation time significant changes were observed in the cell envelope with very translucent membranes due to the leakage of the intracellular content. Therefore, TEMCC induced a membrane photodamage, which was evidenced by a diminished in the osmotic resistance. Membrane fluidization can be due to the formation of membrane defects in the HRB cells caused by photooxidation, which produces the formation of hemolytic holes [23]. This effect on membrane integrity is accompanied by a decrease in the osmotic stability of HRB cells.

3.6. Studies of the photodynamic action mechanism in HRB cells

In order to elucidate the photodynamic mechanism, the effect of sodium azide and mannitol were investigated in the photosensitized damage of the HRB membrane. Thus, sodium azide was used as a quencher of $O_2(^1\Delta_g)$ preventing type II photoprocess, while mannitol was employed as a scavenger of the superoxide anion radical and hydroxyl radical [24,25]. HRB cells were incubated with 50 mM azide ion and this concentration was not hemolytic in the dark or under irradiation without TEMCC (results not shown). In presence of 4 μM TEMCC and light, the addition of azide ion

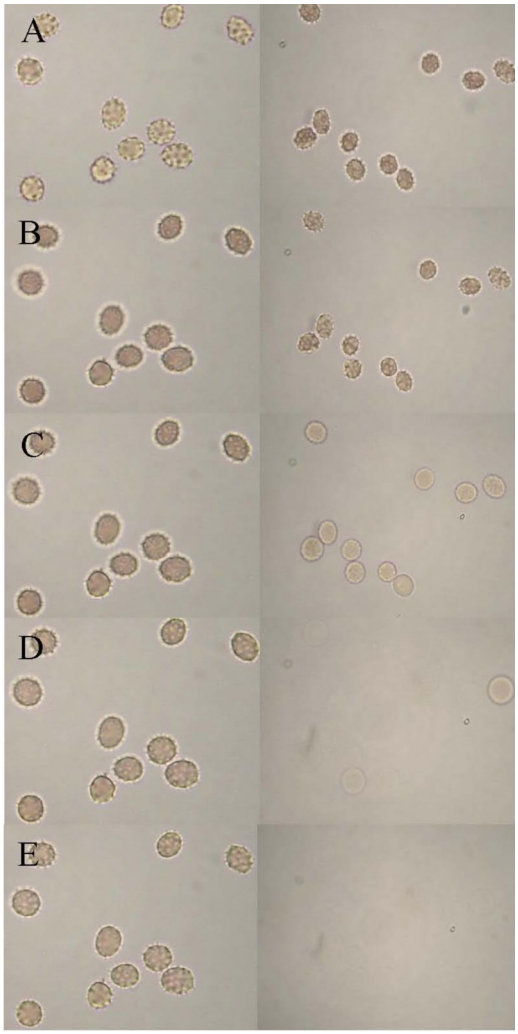

Fig. 8. Microscopic photographs of HRB cells morphology. Control untreated with TEMCC (left column) and treated with 4 μM TEMCC (right column) for 30 min in dark and irradiated with the microscope light source keeping the same field of view for different times (A) 0 min, (B) 5 min, (C) 10 min, (D) 15 min and (E) 20 min; 100× microscope objective.

produced a reduction in the photohemolysis of HRB cells (Fig. 9, line 3). After 5 min of irradiation, the hemolysis percentage of erythrocytes was reduced from 30% to 6%. Therefore, the azide ion quenched the photocytotoxic species, producing a protective effect on HRB cells. Otherwise, the addition of 50 mM mannitol was not toxic for cells in dark. Also, no hemolytic effect was found for cells irradiated in the presence of mannitol (results not shown). In presence of 4 μM TEMCC, photohemolysis percentage was reduced to 4% in the presence of mannitol (Fig. 9, line 4). Thus, photoprotective effect was also observed using mannitol.

On the other hand, the photohemolysis of HRB cells was carried out in D_2O to evaluate the $O_2(^1\Delta_g)$-mediated damage of microbial cells induced by TEMCC. This medium was used to increase the lifetime of $O_2(^1\Delta_g)$ [26]. HRB cells treated with 4 μM TEMCC were not affected in D_2O (0.9%, w/v, NaCl) in dark (Fig. 9, line 6) nor in D_2O (0.9%, w/v, NaCl) under irradiation without photosensitizer (result not shown). However, irradiation of HRB cells incubated with TEMCC in D_2O produced a 70% of photohemolysis, which is considerable higher than that observed in water medium (Fig. 9, line 5).

Therefore, the presence of azide ion produced photoprotection of HRB cells by quenching $O_2(^1\Delta_g)$. This suggests that the

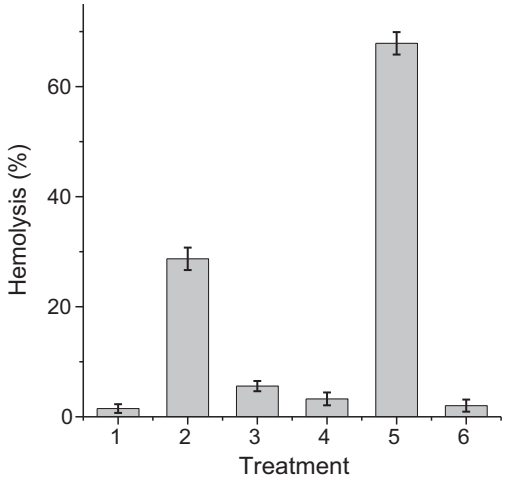

Fig. 9. Photohemolysis of HRB cells (~10^6 cells/mL) treated with 4 μM TEMCC for 30 min in dark in 0.9%, w/v, NaCl solution; (1) cells control in dark; (2) cells irradiated for 5 min; (3) cells containing 50 mM sodium azide and irradiated for 5 min; (4) cells containing 50 mM mannitol and irradiated for 5 min; (5) cells in D_2O and irradiated for 5 min; (6) cells in D_2O and keep in dark. Values represent mean ± standard deviation of three separate experiments.

contribution of $O_2(^1\Delta_g)$ is involved in the photohemolysis of HRB cells. The photohemolytic efficacy of TEMCC was significantly affected when mannitol was added to HRB cells. Also, the photohemolysis of HRB cells was performed in D_2O to evaluate the $O_2(^1\Delta_g)$-mediated. Under this condition, the photocytotoxic effect was higher in D_2O than in aqueous solution. The results reveal a contribution of type II photosensitization in the HRB cell photohemolysis induced by TEMCC. In general, the involvement of $O_2(^1\Delta_g)$ in several photosensitized processes *in vivo* is accepted by an enhancement in D_2O and an inhibition in presence of azide of diverse oxidative reaction rates [24,27,28]. However, photodamage of HRB cells induced by TEMCC was reduced in presence of mannitol. The photoprotective effect produced by mannitol was indicative of some contribution of type I reactions in the inactivation process. Therefore, a type I photochemical mechanism can also be contributing to the photohemolytic activity induced by TEMCC.

4. Conclusions

A *meso*-substituted carbazoyl chlorin TECC was synthesized by diimide reduction of TECP. The reaction produced a chlorin-bacteriochlorin mixture, which was treated with *o*-chloranil to dehydrogenate the bacteriochlorin. Methylation of TECC and TECP was used to obtain tetracationic photosensitizers TEMCC and TEMCP, respectively. Unlike TEMCP, chlorin TEMCC exhibits an intense absorption band in the phototherapeutic window (600–800 nm), emitting red fluorescence. The $O_2(^1\Delta_g)$ production of TEMCC was slightly higher that TEMCP in DMF. In presence of NADH, both photosensitizers produce the reduction of NBT to diformazan. The photohemolytic capacity of these photosensitizers was compared in HRB cells. A higher photohemolytic activity was found for TEMCC in the presence of erythrocytes. The photodynamic action induced by TEMCC was accompanied by a decrease in the HRB cells osmotic stability, which lead to the release of hemoglobin. To elucidate the oxidative processes that occur during the hemolysis of HRB cells, the effect of the azide ion and mannitol was analyzed. Photohemolytic efficacy was affected when mannitol was used as a type I scavenger. Also, photoprotection was found using sodium azide as $O_2(^1\Delta_g)$ quencher, while photohemolysis considerably increased in D_2O, indicating the intermediacy of $O_2(^1\Delta_g)$. Therefore, the present *in vitro* experiments show that TEMCC is a highly effective photosensitizer to produce HRB cells in comparison with its porphyrin homologue. This is mainly due the higher absorption of TEMCC after 600 nm where hemoglobin does not interfere. The photohemolysis induced by TEMCC appears be mediated by a contribution of both type I and type II processes.

Acknowledgments

Authors thank Consejo Nacional de Investigaciones Científicas y Técnicas (CONICET) of Argentina, SECYT Universidad Nacional de Río Cuarto, MINCyT Córdoba and Agencia Nacional de Promoción Científica y Tecnológica (ANPCYT) of Argentina for financial support. M.B.S., M.E.M. and E.N.D. are Scientific Members of CONICET. D.D.F. thanks to ANPCYT for a doctoral fellowship.

References

[1] R.R. Allison, C.H. Sibata, Oncologic photodynamic therapy photosensitizers: a clinical review, Photodiagnosis and Photodynamic Therapy 7 (2010) 61–75.
[2] E.S. Nyman, P.H. Hynninen, Research advances in the use of tetrapyrrolic photosensitizers for photodynamic therapy, Journal of Photochemistry and Photobiology B: Biology 73 (2004) 1–28.
[3] S. Yanoa, S. Hirohara, M. Obata, Y. Hagiya, S. Ogura, A. Ikeda, H. Kataoka, M. Tanaka, T. Joh, Current states and future views in photodynamic therapy, Journal of Photochemistry and Photobiology C: Photochemistry Reviews 12 (2011) 46–67.
[4] P.R. Ogilby, Singlet oxygen: there is still something new under the sun, and it is better than ever, Photochemical & Photobiological Sciences 9 (2010) 1543–1560.
[5] S. Banfi, E. Caruso, S. Caprioli, L. Mazzagatti, G. Canti, R. Ravizza, M. Gariboldi, E. Monti, Photodynamic effects of porphyrin and chlorin photosensitizers in human colon adenocarcinoma cells, Bioorganic & Medicinal Chemistry 12 (2004) 4853–4860.
[6] M.O. Senge, mTHPC-A drug on its way from second to third generation photosensitizer? Photodiagnosis and Photodynamic Therapy 9 (2012) 170–179.
[7] S. Issa, N. Walchshofer, I. Kassab, H. Termoss, S. Chamat, A. Geahchan, Z. Bouaziz, Synthesis antiproliferative activity of oxazinocarbazole and *NN*-bis (carbazolylmethyl)amine derivatives, European Journal of Medicinal Chemistry 45 (2010) 2567–2577.
[8] M.E. Milanesio, M.G. Alvarez, J.J. Silber, V. Rivarola, E.N. Durantini, Photodynamic activity of monocationic and non-charged methoxyphenylporphyrin derivatives in homogeneous and biological media, Photochemical & Photobiological Sciences 2 (2003) 926–933.
[9] L. Kaestner, Evaluation of human erythrocytes as model cells in photodynamic therapy, General Physiology and Biophysics 22 (2003) 455–465.
[10] L. Kaestner, A. Juzeniene, J. Moan, Erythrocytes-the 'house elves' of photodynamic therapy, Photochemical & Photobiological Sciences 3 (2004) 981–989.
[11] J. Durantini, L. Otero, M. Funes, E.N. Durantini, F. Fungo, M. Gervaldo, Electrochemical oxidation-induced polymerization of 5,10,15,20-tetrakis[3-(*N*-ethylcarbazoyl)]porphyrin. Formation and characterization of a novel electroactive porphyrin thin film, Electrochimica Acta 56 (2011) 4126–4134.
[12] M.E. Milanesio, M.G. Alvarez, E.I. Yslas, C.D. Borsarelli, J.J. Silber, V. Rivarola, E.N. Durantini, Photodynamic studies of metallo 5,10,15,20-tetrakis(4-methoxyphenyl)porphyrin: photochemical characterization and biological consequences in a human carcinoma cell line, Photochemistry and Photobiology 74 (2001) 14–21.
[13] Y. Yamakoshi, N. Umezawa, A. Ryu, K. Arakane, N. Miyata, Y. Goda, T. Masumizu, T. Nagano, Active oxygen species generated from photoexcited fullerene (C_{60}) as potential medicines: O_2^- versus $^1O_2$, Journal of the American Chemical Society 125 (2003) 12803–12809.
[14] A. Ikeda, M. Akiyama, T. Ogawa, T. Takeya, Photodynamic activity of liposomal photosensitizers via energy transfer from antenna molecules to [60] fullerene, ACS Medicinal Chemistry Letters 1 (2010) 115–119.
[15] M.B. Spesia, M. Rovera, E.N. Durantini, Photodynamic inactivation of *Escherichia coli* and *Streptococcus mitis* by cationic zinc(II) phthalocyanines in media with blood derivatives, European Journal of Medicinal Chemistry 45 (2010) 2198–2205.
[16] E.A. Dupouy, D. Lazzeri, E.N. Durantini, Photodynamic activity of cationic and non-charged Zn(II) tetrapyridinoporphyrazine derivatives: biological consequences in human erythrocytes and *Escherichia coli*, Photochemical & Photobiological Sciences 3 (2004) 992–998.
[17] M. Pineiro, M.M. Pereira, A.M.D.R. Gonsalves, L.G. Arnaut, S.J. Formosinho, Singlet oxygen quantum yields from halogenated chlorins: potential new photodynamic therapy agents, Journal of Photochemistry and Photobiology A: Chemistry 138 (2001) 147–157.
[18] A. Gomes, E. Fernandes, J.L.F.C. Lima, Fluorescence probes used for detection of reactive oxygen species, Journal of Biochemical and Biophysical Methods 65 (2005) 45–80.

[19] R.W. Redmond, J.N. Gamlin, A compilation of singlet yields from biologically relevant molecules, Photochemistry and Photobiology 70 (1999) 391–475.
[20] M.E. Milanesio, M.G. Alvarez, S.G. Bertolotti, E.N. Durantini, Photophysical characterization and photodynamic activity of metallo 5-(4-(trimethylammonium)phenyl)-10,15,20-tris(2,4,6-trimethoxyphenyl)porphyrin in homogeneous and biomimetic media, Photochemical & Photobiological Sciences 7 (2008) 963–972.
[21] R.S. Covalcante, H. Imasato, V.S. Bagnato, J.R. Perussi, A combination of techniques to evaluate photodynamic efficiency of photosensitizers, Laser Physics Letters 6 (2009) 64–70.
[22] M. Suwalsky, P. Orellana, M. Avello, F. Villena, Protective effect of *Ugni molinae* Turcz against oxidative damage of human erythrocytes, Food and Chemical Toxicology 45 (2007) 130–135.
[23] I.B. Zavodnik, L.B. Zavodnik, M.J. Bryszewska, The mechanism of Zn-phthalocyanine photosensitized lysis of human erythrocytes, Journal of Photochemistry and Photobiology B: Biology 67 (2002) 1–10.
[24] M.A. Rubio, D.O. Mártire, S.E. Braslavsky, E.A. Lissi, Influence of the ionic strength on $O_2(^1\Delta_g)$ quenching by azide, Journal of Photochemistry and Photobiology A: Chemistry 66 (1992) 153–157.
[25] T. Maisch, C. Bosl, R.-M. Szeimies, N. Lehn, C. Abels, Photodynamic effects of novel XF porphyrin derivatives on prokaryotic and eukaryotic cells, Antimicrobial Agents and Chemotherapy 49 (2005) 1542–1552.
[26] F. Wilkinson, W.P. Helman, A.B. Ross, Rate constants for the decay and reactions of the lowest electronically excited singlet state of molecular oxygen in solution. An expanded and revised compilation, Journal of Physical and Chemical Reference Data 24 (1995) 663–1021.
[27] K. Ergaieg, M. Chevanne, J. Cillard, R. Seux, Involvement of both type I and type II mechanisms in Gram-positive and Gram-negative bacteria photosensitization by a *meso*-substituted cationic porphyrin, Solar Energy 82 (2008) 1107–1117.
[28] L.-O. Klotz, K.-D. Kröncke, H. Sies, Singlet oxygen-induced signaling effects in mammalian cells, Photochemical & Photobiological Sciences 2 (2003) 88–94.